Proceedings of the International Gas Turbine Congress 2003 Tokyo
November 2-7, 2003

IGTC2003Tokyo TS-149

The Effects of Specifications of a Fuel Supply Unit with a New Concept for a Dry Low NOx Gas Turbine Combustor

Tsutomu WAKABAYASHI[1], Koji MORIYA[2], Seiichi ITO[2], Shonosuke KOGA[2],
Kazuo SHIMODAIRA[3], Yoji KUROSAWA[3], Kazuo SUZUKI[3] and Osamu KAWAGUCHI[4]

[1]Combustion and Fluid Dynamics TBU, Energy Technology Laboratories
OSAKA GAS CO., LTD.
6-19-9, Torishima, Konohana-ku, Osaka 554-0051, JAPAN
Phone: +81-6-6462-3410, FAX: +81-6-6462-3439, E-mail: twakaba@osakagas.co.jp
[2]OSAKA GAS CO., LTD.
[3]Japan Aerospace Exploration Agency
[4]Keio University

ABSTRACT

This paper describes the effects of specifications of a fuel supply unit with a new fuel supply concept for a dry low NOx gas turbine combustor. From experiments made with a plane model, most of the specifications of the fuel supply elements strongly affected the fuel distribution ratio between the main and pilot regions, which could affect combustion performance.

However, the distribution ratio was hardly changed by the main plates attached at the exit of fuel passage holes, though the fuel distribution in the main region was greatly changed by the plates. From the pressurized combustion test, the main plates decreased NOx emissions at high loads, not affecting any harmful influence on combustion efficiency, BOT, and the pattern factor at high loads. It was estimated that the cause of low NOx could be the uniformity of the equivalence ratio in the main region in the circumferential direction.

INTRODUCTION

The reduction of NOx emissions from stationary gas turbines is necessary to meet the increasingly stringent emissions standards imposed by regulatory agencies worldwide. Current practices involve the injection of water or steam and the use of selective catalytic reduction. These methods have specific limitations and problems, including high installation and operating costs and the requirement of large installation space.

Lean premixed combustion is an effective way to reduce NOx, and development programs for dry low NOx combustors using lean premixed combustion concepts are being actively conducted by several gas turbine manufactures (Solt et al., 1993). However, the stable operating range narrows when this method is applied without any supplementary control. Many techniques have been developed to solve this problem: parallel fuel staging (Aigner et al., 1993; Kitajima et al., 1995; Ishii, 1999; Akita; 1999), series fuel staging (Sato, 1999), and variable geometry systems, such as, inlet guide vane modulation (Smith, 1992), air bleed (Etheridge, 1994), and swirler inlet air control (Smith, 1992; Smith et al., 1991).

However, parallel or series fuel staging requires individual fuel supply devices for each group of burners, and variable geometry systems have problems with reliability and durability, since movable parts are needed in the high-pressure, high-temperature gas stream. Furthermore, neither can respond smoothly to rapid load changes.

In order to solve these problems, a new fuel supply concept has been proposed (Wakabayashi, 2001). This concept uses automatic fuel distribution achieved by an interaction between the fuel jet and the airflow. A schematic diagram of the new concept is shown in Fig. 1. A fuel supply unit is placed at the forward part of a combustor. This unit has an outer main region for lean premixed combustion and an inner pilot region for stable combustion. Fuel is supplied through only one line. A fuel passage hole (b) is located at the outer position of a fuel injection nozzle (a). There is a gap between these parts, and pilot combustion air flows through this gap. At high loads, the fuel jet has so much momentum that it penetrates the airflow through the gap. More fuel is supplied to the main region than to the pilot region and consequently the rate of lean premixed combustion increases. At low loads, the fuel jet has low momentum. More fuel is supplied to the pilot region than to the main region and consequently the combustion becomes stable. Further, this combustion system can offer good response for rapid load changes, because the fuel distribution automatically changes when the load of the gas turbine is changed.

The authors previously assessed the fuel distribution ratio between the main and pilot regions and conducted pressurized combustion tests of a prototype combustor. However, it was not clear to what extent the modifications of the fuel supply element

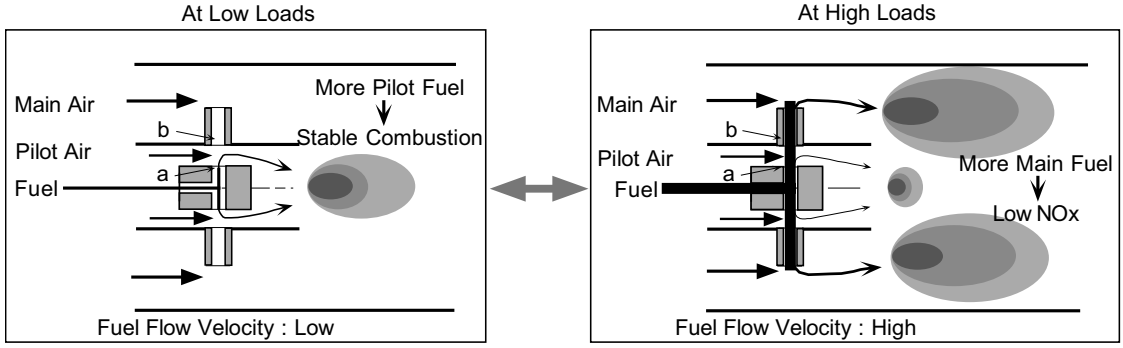

Fig. 1 Diagram of the new fuel supply concept

Copyright (c) 2003 by GTSJ
Manuscript Received on May 6, 2003

specifications would influence the fuel distribution ratio which could affect combustion performance.

This paper describes the effects of modifications of the fuel supply unit specifications on the fuel distribution ratio. In order to examine the fuel distribution ratio when the specifications were modified, such as the gap size, the injected fuel velocity and so on, the authors used a plane flow path model, and examined the fuel distribution ratio in a non-combustion state. Further, pressurized combustion tests of a prototype combustor with a modified fuel supply unit were conducted in order to examine the combustion performance.

FUEL DISTRIBUTION CHARACTERISTICS

Plane Flow Path Model

The plane flow path model is shown in Fig. 2. In order to mainly assess the fuel distribution to the main and pilot regions, there is one of the eight fuel supply elements of the prototype combustor, and the cross-section of the flow path is plane. The shaded portion corresponds to a fuel supply element. The upper region corresponds to the main region, and the lower corresponds to the pilot one. In actual gas turbine combustors, the X direction corresponds to the circumferential direction, Y corresponds to the radial direction, and Z corresponds to the airflow direction.

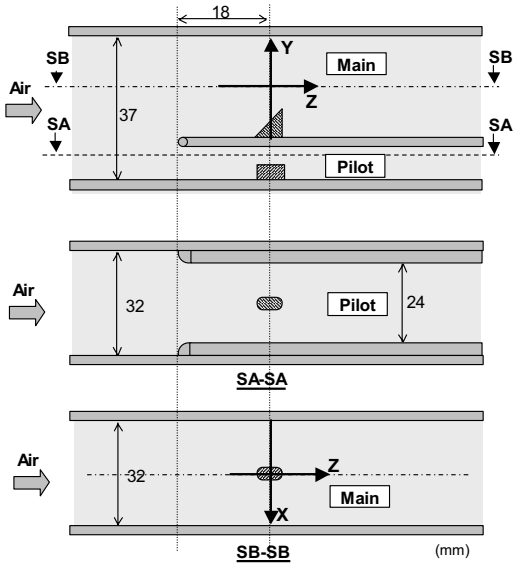

Fig. 2 Structure of the rectangular flow path model. The SA-SA cross-section is in the middle; the SB-SB cross-section is at the bottom.

Specifications of Fuel Supply Elements

One of the fuel supply elements is shown in Fig. 3. Two fuel passage holes are located at the upper part of two fuel injection nozzles. There is a gap between these two parts, and the pilot air flows through this gap. In this model, the following specifications, which could affect the fuel distribution ratio between the main and the pilot regions, are changed:

- Gap size;
- Diameter of the fuel injection nozzles;
- Eccentric length between the fuel passage holes and the fuel injection nozzles; and
- Outer shape of the fuel passage parts.

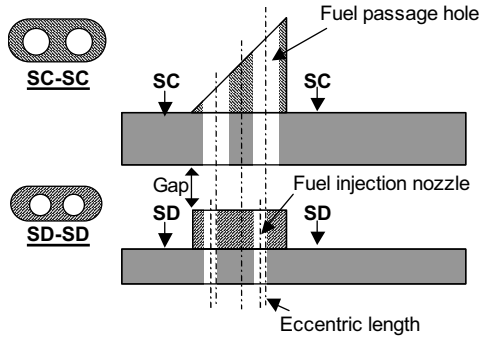

Fig. 3 Structure of a fuel supply element

The specifications of fuel supply elements (types A to H) are shown in Table 1, when the fuel passage holes are made α mm. The diameter of the fuel passage holes for any fuel supply element is the same as that for "A". The outer shapes of fuel passage parts are shown in Fig. 4. All the height of fuel supply passage parts is the same (8.0 mm), and it corresponds to about 30 percent of the height of the main region. A positive value for the eccentric length like the "F" element means that the fuel injection nozzles are set upstream of the fuel passage holes.

The specifications of the modified fuel supply element are shown in Fig. 5. The objective of this modification is that the uniformity of the equivalence ratio in the main region in the X direction (see Fig. 2), which is at a right angle to the airflow direction, is heightened by the main plates at the exit of the fuel passage holes. These main plates function to diffuse the fuel from the fuel passage holes in the X direction. In actual gas turbine combustors, the X direction corresponds to the circumferential direction.

Table 1 Specifications of each fuel supply element

Fuel supply element	The size of a gap	The diameter of fuel injection nozzles	The diameter of fuel passage holes	The eccentric length	The outer shape of fuel passage parts
	mm	mm	mm	mm	
A	0.46 α	0.62 α	α	0.0	Wedge
B	0.31 α	0.62 α	α	0.0	Wedge
C	0.62 α	0.62 α	α	0.0	Wedge
D	0.46 α	0.50 α	α	0.0	Wedge
E	0.46 α	0.42 α	α	0.0	Wedge
F	0.46 α	0.62 α	α	+ 0.19 α	Wedge
G	0.46 α	0.62 α	α	- 0.19 α	Wedge
H	0.46 α	0.62 α	α	0.0	Flat

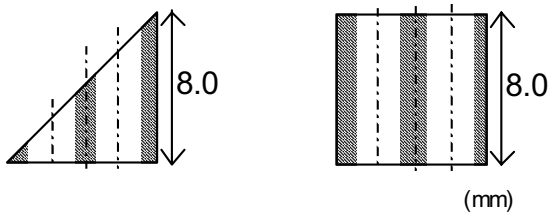

Fig. 4 Structure of the outer shapes of fuel passage parts. The A (Wedge) type is on the left; the H (Flat) type is on the right.

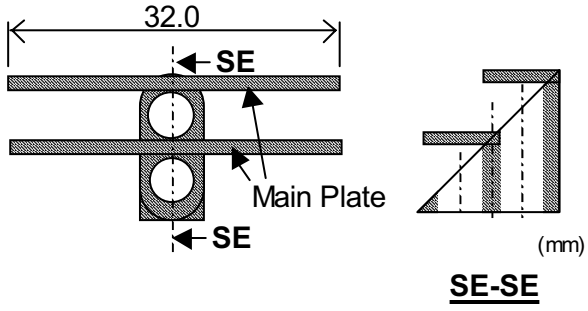

Fig. 5 Structure of modified fuel supply element "J"

Operating Conditions

The operating conditions of the plane model were estimated from the operating conditions of a prototype combustor that the

authors previously manufactured (Wakabayashi, 2001). The operating conditions are shown in Table 2.

The main air flow velocity at the fuel supply element (U_m) was 60 m/s, and the pilot air flow velocity (U_p) was 75 m/s. The air temperature (T) was set to 623 K. These values are almost the same as those for the prototype combustor. However, air pressure in this model (P) was set to 0.13 MPa(A). This value is lower than that in the prototype combustor (0.8 MPa(A)) due to limitations of the experimental apparatus.

The plane model has only one of the eight fuel supply elements of the prototype combustor, in which the maximum total equivalence ratio (including dilution and cooling air) and the air pressure are set to be 0.30 and 0.8 MPa(A), respectively. Therefore, the maximum fuel flow rate in the plane model was decided in consideration of the operating pressure, the number of the fuel supply elements, and the maximum total equivalence ratio of the prototype combustor. Methane (denoted as CH4) and natural gas (denoted as NG, methane: 88%, ethane: 6%, propane: 4%, and butane: 2%) were used as the fuel. In the case of methane, the maximum flow rate in the model was 50.5 NL/min, and in case of natural gas, 43.7 NL/min.

Table 2 Operating conditions in the rectangular model

Main Air Flow Velocity at the Fuel Supply Elements		60 m/s
Pilot Air Flow Velocity at the Fuel Supply Elements		75 m/s
Air Temparature		623 K
Pressure of Air		0.13 MPa(A)
Total Air Flow Rate		1970 NL/min
Max Fuel Flow Rate	Equivalence ratio converted to the prototype combustor	0.30
	(Methane: CH4)	50.5 NL/min
	(Natural Gas: NG)	43.7 NL/min

Experimental Apparatus

The experimental apparatus in the plane model is shown in Fig. 6. Air from the blower was heated to 623 K by the electric heater. The heated air was introduced to the fuel supply elements through the rectification duct, which has a honeycomb grid. The main and pilot lines downstream from the plane flow paths have static mixers to uniform the mixture and orifices to estimate the air distribution ratio between the main and pilot regions. The air distribution was calculated from the air flow rate in each region when fuel was not supplied. The butterfly valve was set only on the main line to adjust the air distribution. Methane and natural gas in gas cylinders were used as fuel. THC and O_2 concentrations in the main and pilot mixtures after the orifices were measured by the gas analyzer in order to calculate the average equivalence ratios in each region.

The fuel distribution ratio was estimated from both the average equivalence ratios in each region and the air distribution ratio.

Moreover, in order to evaluate the distribution of the equivalence ratio in the main region, the sampling probe was set in the main region. The sampling probe has nine holes, each measuring 1.0 mm in diameter.

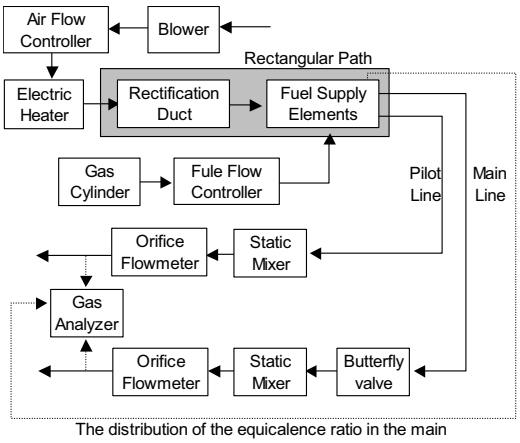

Fig. 6 Experimental apparatus in the plane model

Results and Discussion regarding the Basic Specifications

The fuel distribution ratio to the main region is shown in Fig. 7 when the gap size was changed. The gap size of the "A" element is 0.46 α mm, "B" is 0.31 α mm, and "C" is 0.62 α mm. The horizontal axis is the total equivalence ratio converted to a prototype combustor (ϕ_t). As the gap size becomes larger, the fuel distribution ratio becomes lower and the minimum equivalence ratio at which the fuel is started to be supplied to the main region (ϕ_s) becomes higher. The effect of the gap size to ϕ_s was almost linear.

The fuel distribution ratio to the main region is shown in Fig. 8 when the diameter of the fuel injection nozzles, which relate the fuel injection velocity, was changed. The diameter of the "A" element is 0.62 α mm, "D" is 0.50 α mm, and "E" is 0.42 α mm. If

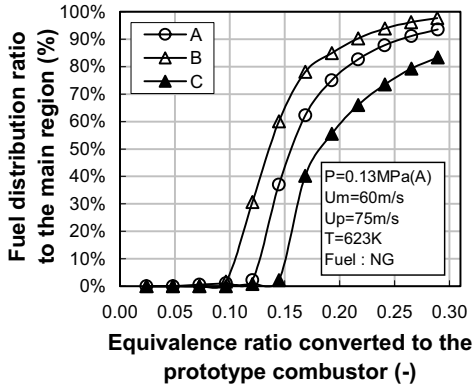

Fig. 7 Fuel distribution ratio for different gap sizes

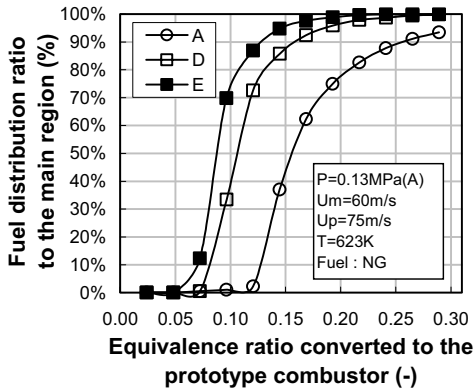

Fig. 8 Fuel distribution ratio for different diameters of the fuel injection nozzles

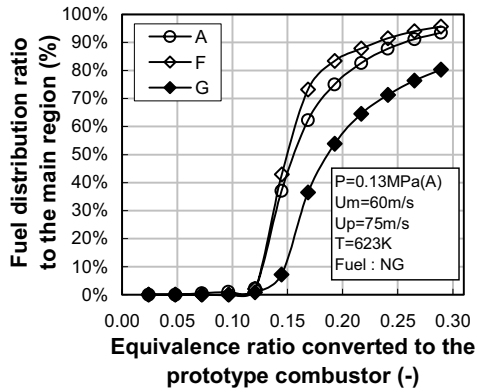

Fig. 9 Fuel distribution ratio for different eccentric lengths

the reciprocal number of the fuel injection cross-section of the "A" element is 100%, the reciprocal numbers of "D" and "E" become 150% and 200%, respectively. As the diameter of the fuel injection nozzles becomes larger, the fuel distribution ratio becomes lower and the ϕ_s becomes higher. The effect of the reciprocal number of the fuel injection cross-section to ϕ_s was not linear.

The fuel distribution ratio to the main region is shown in Fig. 9 when the eccentric length between the fuel passage holes and fuel injection nozzles was changed. A positive value for the eccentric length like the "F" element means that the fuel injection nozzles are set upstream of the fuel passage holes. The ϕ_s of the "F" element is almost the same as that of "A". However, the ϕ_s of "G" is much higher than that of "A". The fuel distribution ratio to the main region of "F" is slight higher than that of "A". However, the fuel distribution ratio to the main region of "G" is much lower than that of "A".

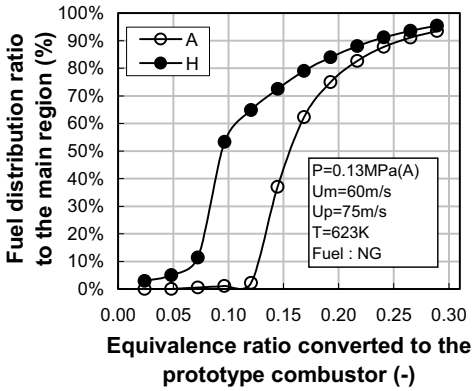

Fig. 10 Fuel distribution ratio for different passage parts

The fuel distribution ratio to the main region is shown in Fig. 10 when the outer shape of fuel passage parts was changed, such as A (Wedge) and H (Flat). In the case of the "H" element, fuel is easily supplied to the main region. It is estimated that the main air might eject fuel in the case of "H", while the main air presses the fuel in the case of "A". However, the fuel distribution ratio of "H" at ϕ_t of 0.30 was almost the same as that of "A".

Most of the specifications of the fuel supply elements, such as the gap size, diameter of the fuel injection nozzles, eccentric length between the fuel passage holes and fuel injection nozzles, and the outer shape of the fuel passage holes strongly affect the fuel distribution ratio between the main and pilot regions, which could affect combustion performance.

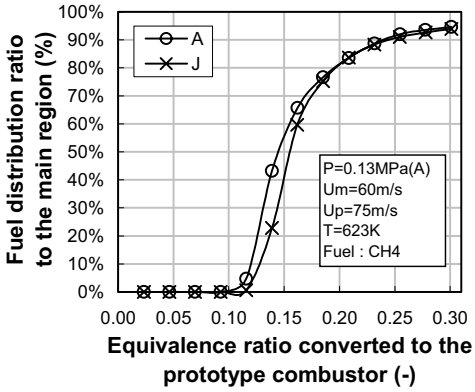

Fig. 11 Fuel distribution ratio of the modified fuel supply element

Results and Discussion regarding the Modified Specifications

The fuel distribution ratio to the main region of the modified fuel supply element "J" is shown in Fig. 11. The main objective of this modification is that the uniformity of the equivalence ratio in the main region in the X direction is heightened. This was a result of using methane. The ϕ_s of the "J" element is slightly higher than that of "A". It is estimated that the main plates in "J" became an obstacle to the fuel supply to the main region. However, the fuel distribution ratio of "J" at ϕ_t of 0.30 was almost the same as that of "A". This tendency of methane was not different from that of natural gas. Thus, this modification hardly affects the fuel distribution ratio to the main region.

Next, the distributions of the equivalence ratio in the main region at ϕ_t of 0.30 are shown in Figs. 12 and 13. The fuel is methane. The coordinate axes are shown in Fig. 2.

Figure 12 shows the Y-axis distribution of "A" and "J" elements at Z=20 mm, 70 mm and 120 mm (X=0 mm). A few data of "A" at Z=20 mm are not displayed because the THC

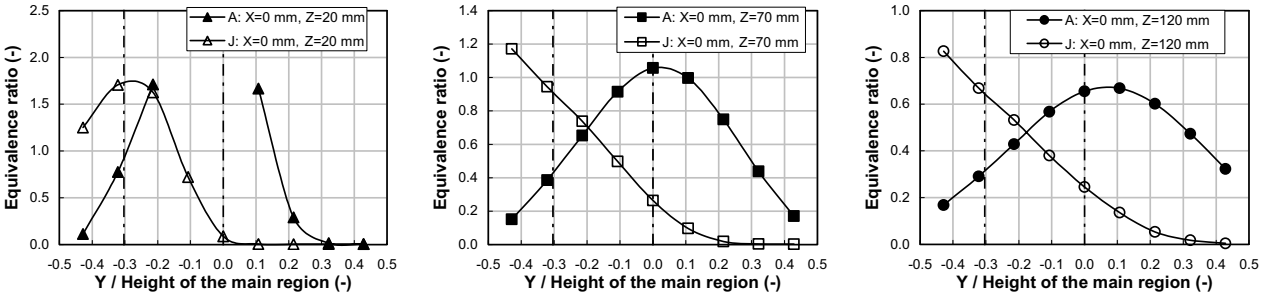

Fig. 12 Equivalence ratio in the main region in the Y-axis direction. The left figure is at Z=20 mm, middle at Z=70 mm, and right at Z=120 mm.

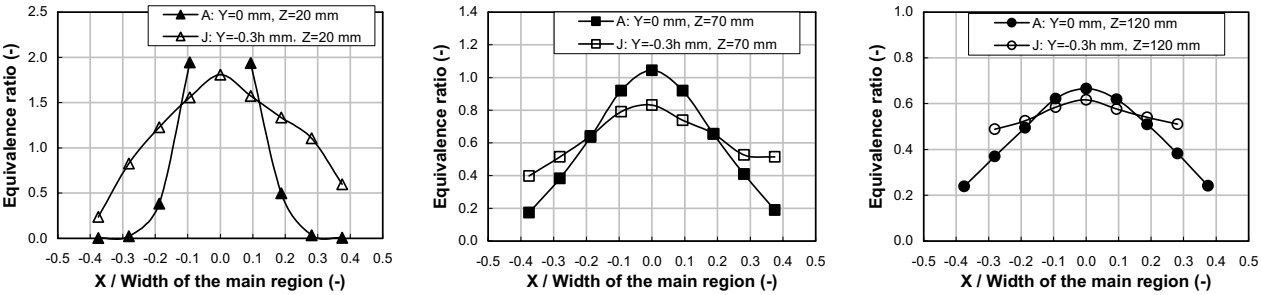

Fig. 13 Equivalence ratio in the main region in the X-axis direction. The left figure is at Z=20 mm, middle at Z=70 mm, and right at Z=120 mm.

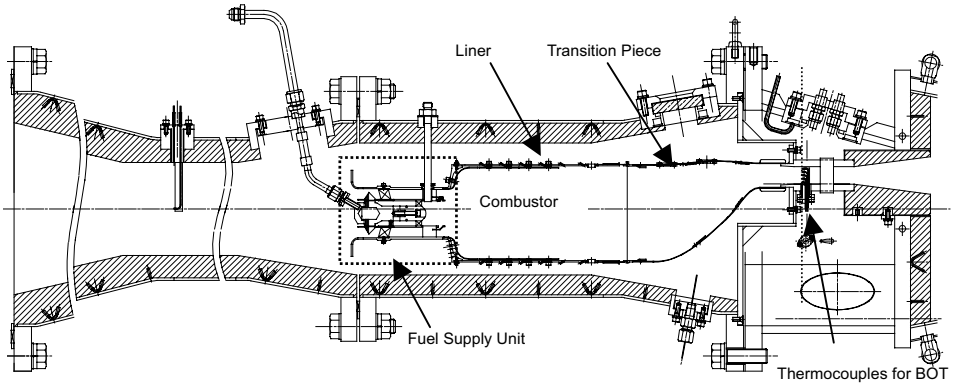

Fig. 14 Cross-section of the prototype combustor and test rig

concentrations were over the maximum measurement range of 20%. In the case of "J", the equivalence ratio on the bottom side is higher than that on the topside. The maximum equivalence ratio of "J" at Z=120 mm is a little higher than that of "A". If the flow rate in each area is not considered, this modification of "J" may increase NOx.

Figure 13 shows the X-axis distribution of "A" and "J" elements at Z=20 mm, 70 mm and 120 mm. When the height of the main region is made *h*, the measurement position of "A" and "J" are Y=0 mm and Y= –0.3 *h* mm, at which the equivalence ratios are comparatively high. A few data of "A" at Z=20 mm are not displayed because the THC concentrations were over the maximum measurement range of 20%. At Z=20 mm, the fuel in "J" was distributed in a wider area than in "A". Therefore, at Z=120 mm, the uniformity of the equivalence ratio of "J" is much higher that of "A". If the flow rate in each area is not considered, this modification of "J" could decrease NOx.

Therefore, if the effect of the uniformity of the equivalence ratio in the X direction (the circumferential direction in an actual combustor) is much stronger than that of the increase of equivalence ratio in the Y direction (the radial direction in an actual combustor), it is possible that the modification of "J" can function to decrease NOx at high loads. Therefore, a pressurized combustion test of a modified fuel supply unit like "J" was conducted.

COMBUSTION CHARACTERISTICS

Structure of Combustor and Test Rig

Figure 14 shows a cross-section of the prototype combustor and the test rig. This combustor is one of six can-annular type combustors (4000 kW class). The maximum equivalence ratio is set to 0.30. This combustor has a fuel supply unit, a liner (ID: 142.3 mm) and a transition piece.

Figures 15 and 16 show the details of the fuel supply unit and the fuel supply element. Two fuel passage holes (b) are located at the outer part of two fuel injection nozzles (a). There is a gap between both parts, through which the pilot combustion air flows. These devices were positioned axially at each of eight locations arranged in a circle. At the exit of the fuel passage hole of "J", cylindrical plates denoted as main plates are also attached. The "A" fuel supply unit does not have any main plates. The picture of the fuel supply unit with the main plates from the upstream view is shown in Fig. 17.

Experimental Apparatus and Conditions

The pressurized combustion test facility is shown in Fig. 18. Taking actual gas turbine operating conditions into consideration, the inlet air temperature (T) was 623 K and the air volume flow velocity at the liner (U_c), defined as the value that the air volume flow (including dilution and cooling air) was divided by the cross-section of the liner, was 24 m/s, and the compressor discharge pressure (P) was 0.8 MPa(A). Natural gas was used as the fuel.

The concentrations of NOx, O_2, CO, CO_2 and UHC in the exhaust gas were measured by standard gas analysis procedures. A water-cooled sampling probe was mounted at a location about 1 m downstream from the combustor exit. This probe was designed to mix equal amounts of exhaust gas sampled from seven holes, each measuring 1.0 mm in diameter. The combustion efficiency and total equivalence ratio (ϕ_t) were calculated from the measured exhaust gas compositions.

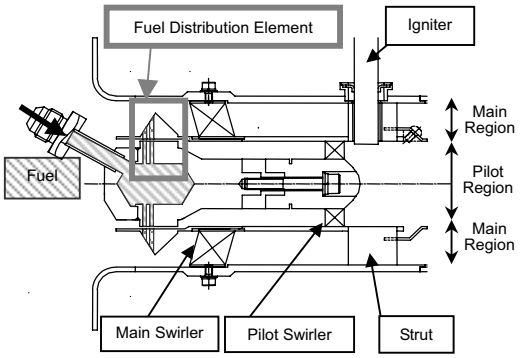

Fig. 15 Structure of the fuel supply unit

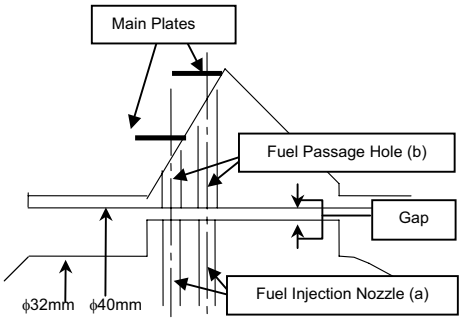

Fig. 16 Structure of the fuel supply element

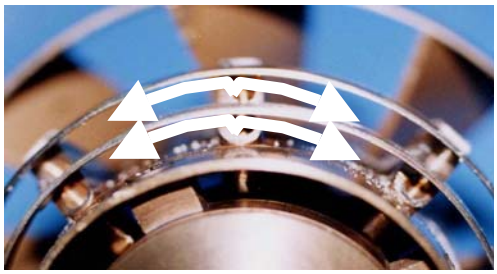

Fig. 17 Picture of the fuel supply unit with the main plates from the upstream view (J)

The average temperature of the exhaust gas at the combustor exit, called the BOT (burner outlet temperature), was measured by 50 thermocouples (R-type, Inconel sheath, 1.6 mm in diameter, see Fig. 14).

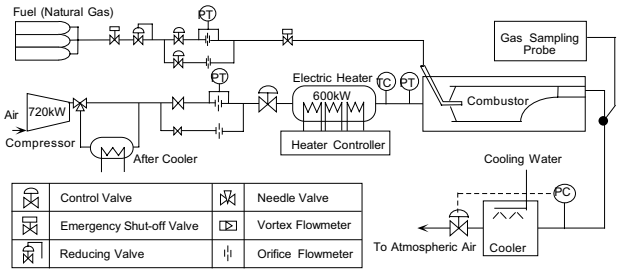

Fig. 18 Pressurized test facility

Results and Discussion

Figure 19 shows the correlation between NOx emissions (at 15% O_2) and ϕ_t. The NOx of each combustor begins to decrease over ϕ_t of 0.15, and in the range of ϕ_t up to 0.2, the NOx of "J" is almost the same as that of "A". However, over ϕ_t of 0.2, as the ϕ_t becomes higher, the NOx of "J" becomes lower compared to that of "A". At ϕ_t of 0.28, the NOx of "J" is 2/3 of that of "A". The reason for this performance is estimated as follows: From the experimental results of the plane model, more fuel is supplied to the pilot region than to the main region in the range of ϕ_t up to 0.15. Conversely, more fuel is supplied to the main region than to the pilot region over ϕ_t of it. Therefore, as the ϕ_t becomes higher, the NOx of each combustor becomes lower. Furthermore, in the range of high ϕ_t, like over 0.2, it is considered that the effect of uniformity of the equivalence ratio in the circumferential direction generates much more strongly than that of the increase in the equivalence ratio in the radial direction by the attachment of the main plates. Therefore, in the range of high ϕ_t, the NOx of "J" is lower than that of "A".

Figure 20 shows the correlation between the combustion efficiency and ϕ_t. In the range ϕ_t from 0.20 to 0.28, as the ϕ_t becomes lower, the combustion efficiency becomes lower. However, even if ϕ_t decreases in the equivalence ratio of 0.15 to 0.20, the combustion efficiency does not decrease. The reason for this is assumed to be that, in this range, the fuel distribution ratio to the pilot region increases intensely when ϕ_t decreases from the experimental results of the plane model. Therefore, stable combustion is achieved at low loads, and the combustion efficiency does not decrease. Moreover, only in the range of ϕ_t from 0.15 to 0.20, the combustion efficiency of "J" is slightly higher than that of "A". It is considered that the main plates of "J" become an obstacle to the fuel supply to the main region, so the combustion in the pilot region is stronger. However, the combustion efficiency is low, especially around ϕ_t of 0.10. Since fuel is supplied only to the pilot region under ϕ_t of 0.15, the modification of the pilot specification could improve the combustion efficiency. This improvement is our next task.

Figure 21 shows the correlation between BOT (burner outlet temperature) and ϕ_t. The BOT of "J" is almost the same as that of "A". Furthermore, the pattern factor of "J" over ϕ_t of 0.25, which is important to the durability of 1st vanes, was less than 0.13, and almost the same as that of "A".

Therefore, it is considered that the main plates decreased NOx emissions at high loads, and did not cause any harmful influence on combustion efficiency, BOT, and the pattern factor at high loads. It is estimated that the cause of low NOx at high loads could be the uniformity of the equivalence ratio in the main region in the circumferential direction.

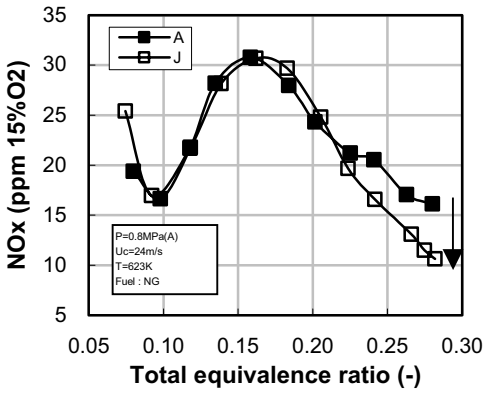

Fig. 19 NOx emissions

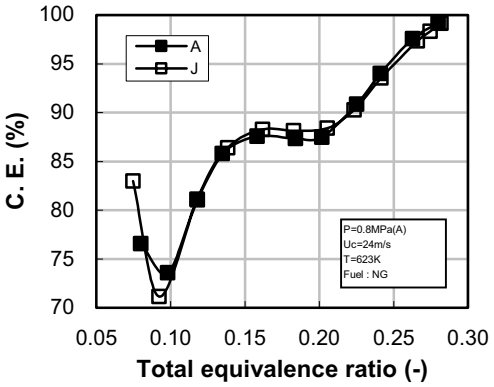

Fig. 20 Combustion efficiency

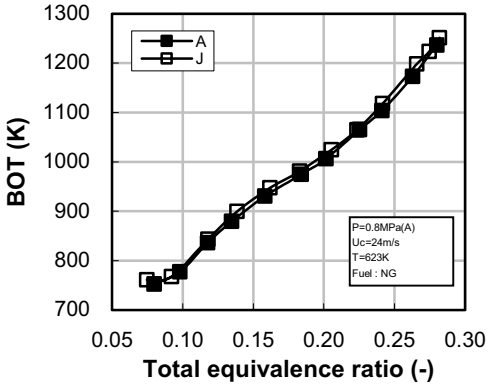

Fig. 21 BOT

CONCLUSION

The effects of specifications of the fuel supply unit with a new fuel supply concept for a dry low NOx gas turbine combustor on fuel distribution were evaluated using a plane model.

Most of the specifications of the fuel supply elements, such as gap size, diameter of the fuel injection nozzles, eccentric length between the fuel passage holes and fuel injection nozzles, and outer shape of the fuel passage holes strongly affect the fuel distribution ratio between the main and pilot regions, which could affect combustion performance.

However the distribution was hardly changed by the main plates attached at the exit of the fuel passage holes, though the fuel distribution in the main region was greatly changed by the plates. From the pressurized combustion test using a prototype combustor, the main plates decreased NOx emissions at high loads, and did not cause any harmful influence on combustion efficiency, BOT, and the pattern factor at high loads. It is estimated that the cause of low NOx at high loads could be the uniformity of the equivalence ratio

in the main region in the circumferential direction from experiments with the plane model.

REFERENCES

Aigner, M., and Muller, G., 1993, "Second-Generation Low-Emission Combustors for ABB Gas Turbines: Field Measurements with GT11N-EV," *ASME Journal of Engineering for Gas Turbine and Power*, Vol. 115, pp. 533-536.

Akita, E., and Nishida, M., 1999, "Development and Verificational Operation of 1500C Class Next Generation High Efficient G series Gas Turbine," *Journal of the Gas Turbine Society of Japan*, Vol. 27, No. 3, pp. 138-145.

Etherdge, C. J., 1994, "Mars SoLoNOx-Lean Premix Combustion Technology in Production," ASME 94-GT-255.

Ishii, J., 1999, "The Next Generation High-Efficiency Combined-Cycle Power Plants which used 1500C-class Steam Cooled Gas Turbine," *Journal of the Gas Turbine Society of Japan*, Vol. 27, No. 3, pp. 161-165.

Kitajima, J., Kimura, T., Sasaki, T, Okuto, A., Kajita, S., Ohga, S., and Ogata, M., 1995, "Development of a Second Generation Dry Low NOx Combustor for 1.5MW Gas Turbine," ASME 95-GT-255.

Sato, H., Amano, T., Iiyama, Y., Mori, M., and Nakamura, T., 1999, "Development of a Three-Staged Low Emissions Combustor for Industrial Small-Size Gas Turbines," ASME 99-GT-236.

Smith, K. O., Holsapple, A. C., Mak, H. K., and Watkins, L., 1991, "Development of a Natural Gas Fired, Ultra-Low NOx Can Combustor for 800 kW Gas Turbine Engines," ASME 91-GT-303.

Smith, K. O., 1992, "Engine Testing of a Prototype Low NOx Gas Turbine Combustor," ASME 92-GT-116.

Solt, J. C., and Tuzson, J., 1993, "Status of Low NOx Combustor Development," ASME 93-GT-270.

Wakabayashi, T., Ito, S., Koga, S., Ippommatsu, M., Moriya, K., Simodaira, K., Kurosawa, Y., and Suzuki, K., 2001, "Performance of a dry low-NOx gas turbine combustor designed with a new fuel supply concept," *ASME Journal of Engineering for Gas Turbine and Power*, Vol. 124, pp. 771-775.